Validating rapid InSAR subsidence rates in Tehran, Iran using laser altimetry data and VHR DEMs

Jess Payne*[1], Andrew Watson[1], Scott Watson[1], John Elliott[1]

*eejap@leeds.ac.uk

[1]COMET, University of Leeds

1. The Problem

Iran is an arid country with few surface water stores. Groundwater pumping rates are currently used to provide freshwater for agriculture and industry. Natural groundwater recharge rates cannot keep pace with extraction rates, leading to land subsidence observable by satellites.

Iran experiences some of the fastest land subsidence rates in the world at over 150 mm/yr.

We use Sentinel-1 InSAR data 2014-2022 and COMET LiCS processing tools [1,2] to calculate subsidence rates across Iran at 100 m resolution.

It is difficult to validate these InSAR velocities due to a sparsity of three-component GNSS stations in Iran (Figure 1, [3]).

Validation is important as different interferogram unwrapping spproaches lead to different calculated vertical subsidence rates.

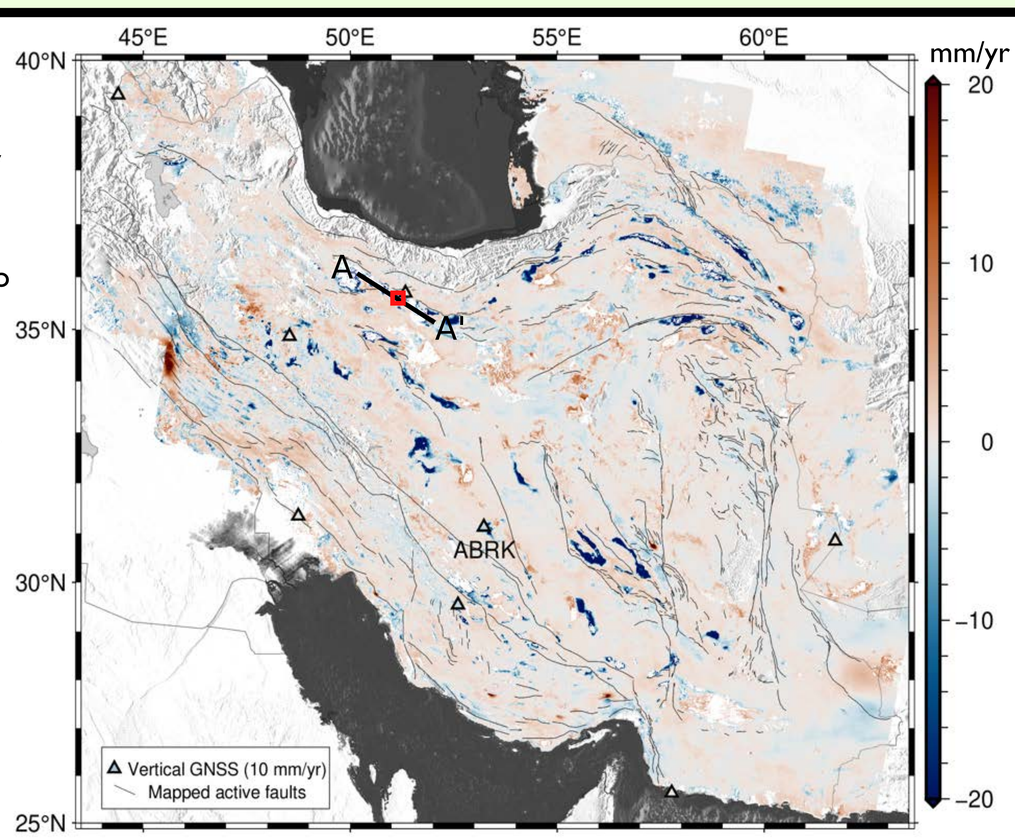

***Figure 1**: Vertical Sentinel-1 InSAR velocities (2014-2020 [4]) and vertical open-access GNSS velocities [3] across Iran. Blue is moving down, red is up. Line-of-sight (LoS) velocities A-A' plotted in Fig. 2. Red box is region in Fig. 5.*

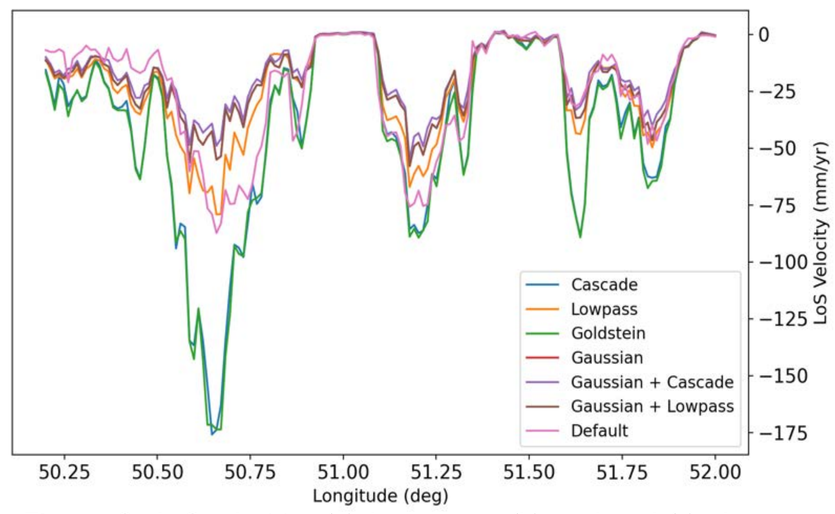

***Figure 2**: LoS velocities (a), loop errors (b), and vstd (c) along A-A', Fig. 1. Calculated using LiCSBAS time-series analysis tools [2]. Line colours indicate interferogram uwrapping method.*

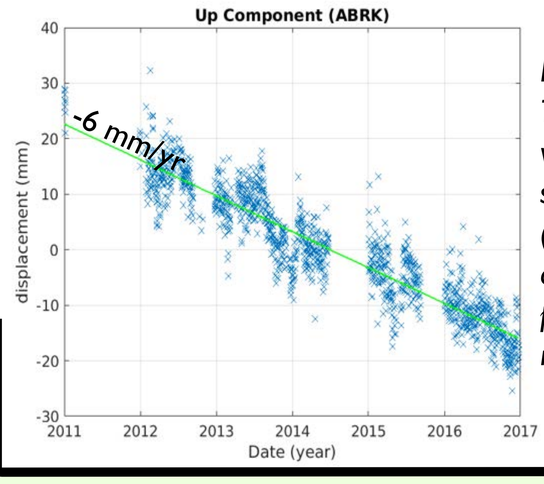

***Figure 3 (left)**: Time-series of fastest vertically moving GNSS station in Iran, ABRK [3] (Fig. 1). GNSS stations are not optimally positioned to record rapid land subsidence.*

2a. Solution A?

ICESat and ICESat-2 Laser Altimetry

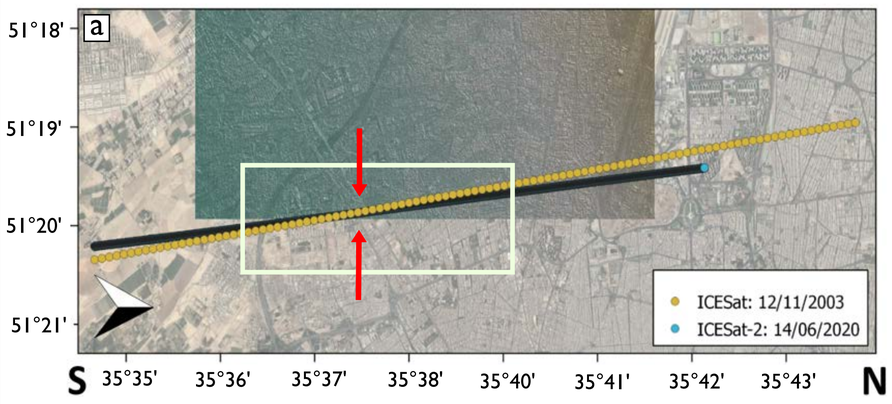

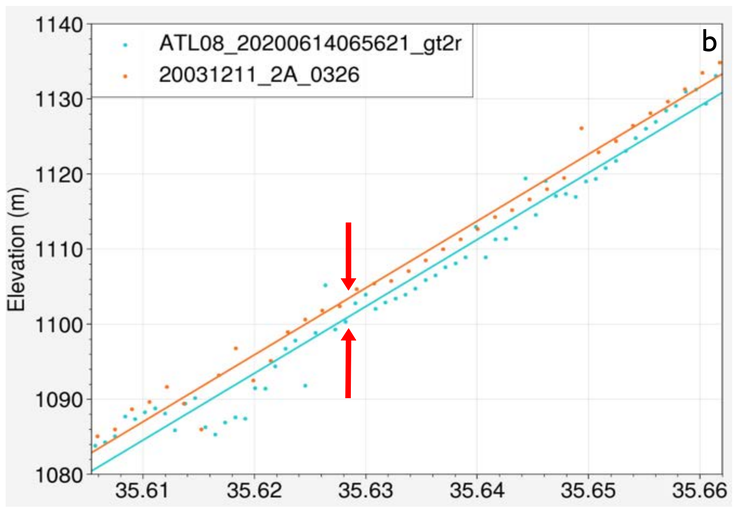

***Figure 4:** Selected ICESat and ICESat-2 (here ATL08 [5]) track data over SW Tehran (a). Box highlights area in b. (b) Polynomials fit to altimetry products. Red arrows point to exact location of track intersection. Orange is ICESat, blue is ICESat-2.*

Method

1. Find ICESat and ICESat-2 tracks that cross in AOI (a)
2. Download ICESat elevation product and ICESat-2 ATL03 and ATL08 [5] products. Inspect quality of data.
3. Filter ATL03 photons by confidence, if using.
4. Fit polynomial to track data (b).
5. Difference polynomials to calculate displacement (b).

2b. Solution B?

*to be analysed

Very High Resolution (VHR) Digital Elevation Models (DEMs)

Acquisition	Sensor	Resolution	Stereo
2012	Pléaides	50 cm	Bi-stereo
2014	Pléaides	50 cm	Tri-stereo
2016	Pléaides	50 cm	Bi-stereo
2022	Pléaides Neo	30 cm	Tri-stereo
2023*	Pléaides Neo	30 cm	2 x Tri-stereo

1. Construct 1 m DEMs using panchromatic (tri-) stereo sets for each acquisition above using Agisoft Metashape. Use point cloud data with confidence >1.
2. Regrid and difference DEMs using xdem python package.

3a. Results A

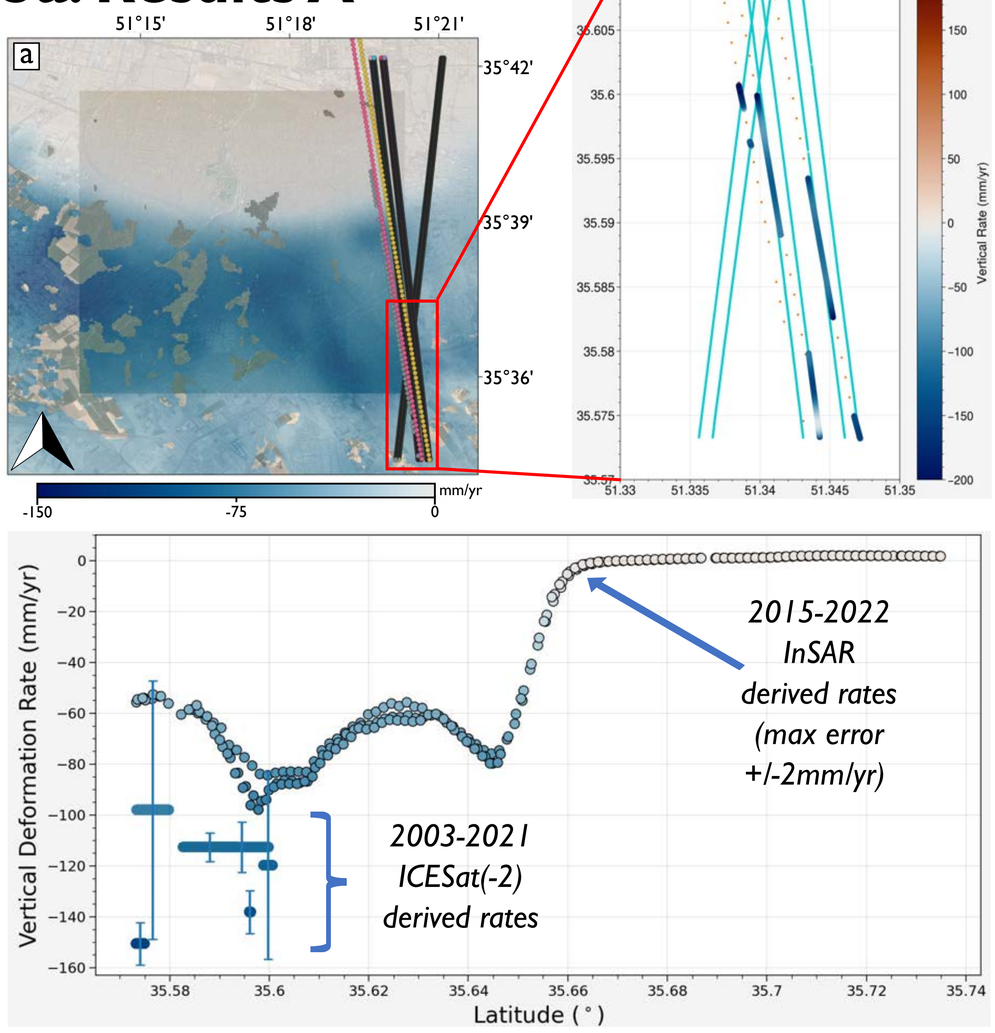

***Figure 5 (left):** (a) Vertical InSAR velocities, SW Tehran (box, Fig. 1) overlain with ICESat(-2) tracks used to calculate vertical rates. DEM extent plotted underneath (Fig 7). (b) ICESat data plotted in orange, ICESat-2 in light blue. Displacement rates at track intersections overlain.*

***Figure 6 (left):** Resulting mean vertical deformation rates calculated using ICESat(-2) topographic differencing compared to Sentinel-1 vertical subsidence rates in the same region.*

3b. Results B

VHR DEM Differencing

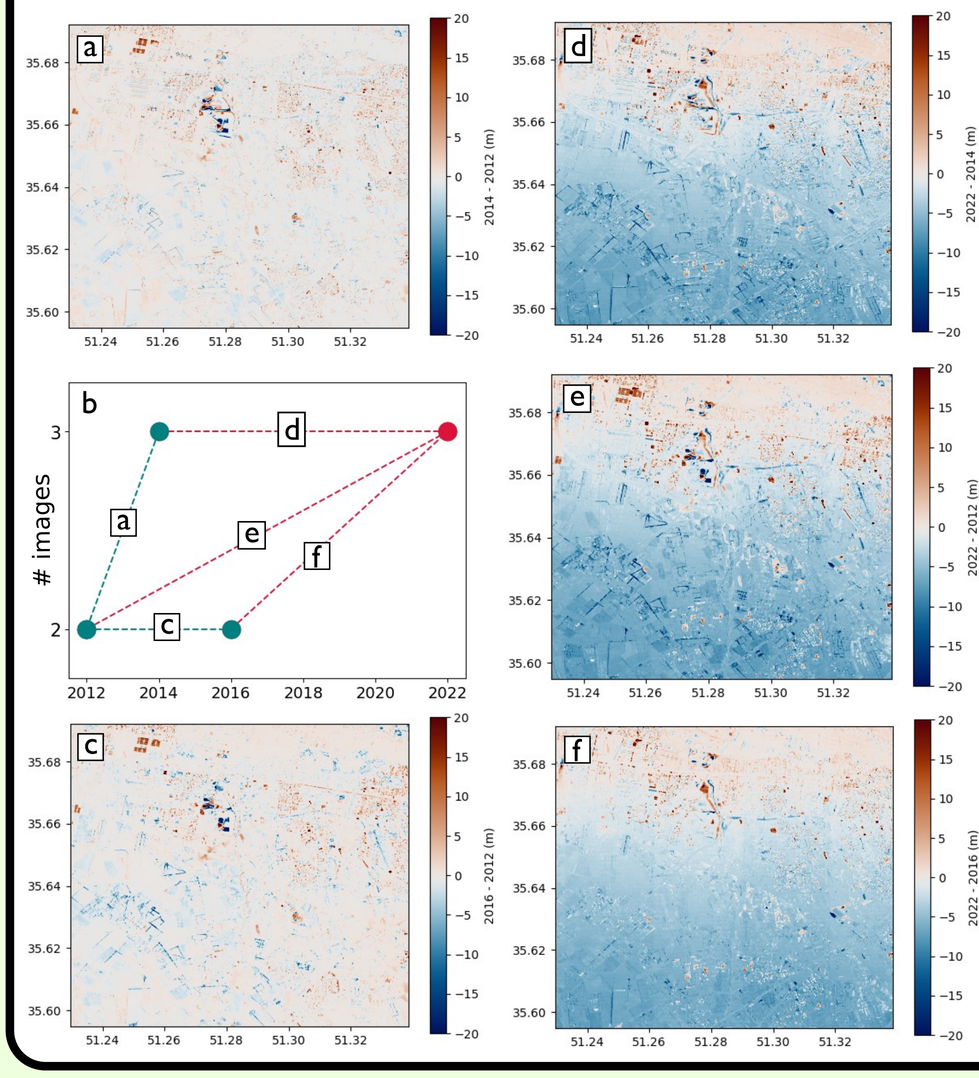

***Figure 7 (right):** DEM differences highlight fastest subsidence in SW of the AOI (a) as expected from InSAR results (Fig. 5). Subsidence magnitude (vertical change) increases with time (c). A ramp artefact remains to be removed from differences that include Pléiades Neo 2022 DEM (d, e, f).*

4. Future Work

- Test methods to remove ramp artefact from Pléiades Neo differences
- Difference laser altimetry data and VHR DEMs
- Process Pléiades Neo 2023 double tri-stereo data (6 images)
- Incorporate other tools e.g. SlideRule

5. References

[1] Lazecký, M., et al., (2020). Remote Sensing, 12 (15), 2430.
[2] Morishita, Y. et al., (2020). Remote Sensing, 12 (3), 424.
[3] Blewitt, G., et al., (2018). Eos, 99.
[4] Watson, A. et al., (2022). JGR: Solid Earth, 127 (2).
[5] Neuenschwander, A., et al., (2020). NASA NSIDC Active Archive Center.